International Journal of Thermal Sciences 48 (2009) 1748–1754

Contents lists available at ScienceDirect

International Journal of Thermal Sciences

journal homepage: www.elsevier.com/locate/ijts

# Periodical heat transfer in parallel-plate channel of improved flow-inclining inserts

J.G. Jiang, Z.X. Yuan*, G.D. Xia

*College of Environmental and Energy Engineering, Beijing University of Technology, Chao Yang District, Ping Le Yuan 100, Beijing 100124, China*

ARTICLE INFO

*Article history:*
Received 6 May 2008
Received in revised form
8 February 2009
Accepted 9 February 2009
Available online 23 March 2009

*Keywords:*
Enhancement
Quasi-streamlined insert
Field synergy
Convection

ABSTRACT

The convective heat transfer and the flow resistance in the 2-D channel with quasi-streamlined insert have been numerically studied in the periodically fully developed regime. The range of the Reynolds number covers both the laminar and the turbulent flow. The effect of the insert angle, the plate thickness vs the Reynolds number on the heat transfer and the friction factor has been identified. The heat transfer gets stronger monotonically with the insert angle from 0° to 30°. Nevertheless, the insert angle impacts the flow resistance in the laminar case much less than in the turbulent case. The combined analysis indicates that the thicker insert is suitable to use in the laminar flow and the thinner insert suitable to the turbulent flow. In any case, the quasi-streamlined insert acts as an upgrader to the local heat transfer coefficient. In comparison with the effect of the original straight flow-inclining insert, the streamlined insert largely diminishes the flow resistance but with only moderate deterioration of the heat transfer. The assessment under the identical pump power consumption reveals the superiority of the improved streamline insert to the straight one.



## 1. Introduction

The efficient performance of thermal equipment often depends on the heat transfer rate involved in it. The process of heat transfer is a typical nonreversible process. The enhancement of heat transfer means diminishing the nonreversible loss, in that for an enhanced structure a less temperature difference is needed to transfer the same amount of heat. In addition, the heat transfer enhancement is often related to the miniaturization of thermal system and the pollution control of exhaust, so that the theory and technique of heat transfer enhancement have continuously drawn attention from the scientific and technical circles. For heat transfer process that involves fluid flow, the convective thermal resistance between the fluid and the wall often constitutes the main part of the entire thermal resistance. Therefore, research on the enhancement of convection heat transfer has been a hot topic in the past years.

For long time the people know that changing the flow direction or disturbing the fluid near the duct wall is helpful to improve the heat transfer rate. Based on the concept of destroying the flow boundary layer, many enhanced configurations such as spirally fluted tube [1], and ducts with rod disturbances [2,3] or short disturbing inserts [4], have been developed and studied. At the same time when those configurations gained the enhancement effect, the resulted pressure-drop penalty was often significant. Guo and his co-workers analyzed the process of heat transfer in the boundary layer with a different view [5,6]. They derived an equation reflecting the relation of the wall heat flux, the fluid velocity and the temperature gradient of the fluid as

$$\rho C_p \int_0^{\delta} (\vec{U}\cdot\nabla\vec{T})\mathrm{d}y = -\lambda\frac{\partial T}{\partial y}\Big|_w = q_w \qquad (1)$$

This relation is called the Principle of Field Synergy (PFS). The relation shown in Eq. (1) indicates that the heat flux on the wall depends not only on the fluid velocity itself, but also on the included angle between the velocity and the temperature gradient. Tao et al. extended this relation into the parabolic flow [7]. Based on the PFS, Wang et al. proposed three new approaches to enhance the convective heat transfer [6]: (1) use of gradually constricting duct, (2) reasonable variation of thermal boundary condition, and (3) use of specially designed inserts. The optimization of thermal boundary condition for enhancement purpose was discussed in Ref. [8]. Some novel enhanced configurations have also been developed according to the PFS [9,10].

As an application of the PFS, the heat transfer in the channel with 2-D and 3-D flow-inclining inserts has been numerically and experimentally studied by the present author [10,11]. As the

* Corresponding author. Tel.: +86 10 67396661; fax: +86 10 67392774.
*E-mail addresses:* zxyuan16@yahoo.com.cn, zxyuan@bjut.edu.cn (Z.X. Yuan).

1290-0729/$ – see front matter © 2009 Elsevier Masson SAS. All rights reserved.
doi:10.1016/j.ijthermalsci.2009.02.001

**Nomenclature**

| | |
|---|---|
| $b$ | thickness of the insert, mm |
| $C_p$ | specific heat, J/kg K |
| $D_e$ | equivalent diameter of the duct, m |
| $f$ | friction factor |
| $h$ | heat transfer coefficient, W/m$^2$ K |
| $H$ | half duct height, mm |
| $k$ | thermal conductivity, W/m K |
| $K$ | turbulent kinetic energy, J/kg |
| $L$ | length of a cycle, mm |
| $Nu$ | Nusselt number |
| $P$ | pressure, Pascal |
| $q$ | heat flux, W/m$^2$ |
| $Re$ | Reynolds number |
| $T$ | temperature, K |
| $\nabla T$ | temperature gradient, K/m |
| $u$, $v$ | velocity component, m/s |
| $\vec{U}$ | velocity vector, m/s |
| $x$, $y$ | Cartesian coordinate, mm |

*Greek symbols*

| | |
|---|---|
| $\beta$ | inclining angle of the insert, ° |
| $\delta$ | thermal boundary layer thickness, m |
| $\varepsilon$ | turbulent dissipation rate, W/kg |
| $\nu$ | kinematic viscosity, m$^2$/s |
| $\rho$ | fluid density, kg/m$^3$ |

*Subscripts*

| | |
|---|---|
| 0 | smooth duct |
| m | mean |
| w | wall |

continuous work to the previous study, a kind of quasi-streamlined flow-inclining insert shown in Fig. 1 is proposed to substitute the original straight insert in Refs. [10,11], so that better enhancement effect will be reached. As it is revealed in Refs. [10,11], the drastic deformation of the fluid streams at the leading and trailing edges of the straight insert results in great pressure-drop. The usage of the streamlined insert is hoped to alleviate this pressure penalty in such kind of enhanced structure. The numerical simulation will focus on the effect of the insert angle $\beta$ and the plate thickness $b$ on the flow and heat transfer characteristics. The involved Reynolds number covers both the laminar flow and the turbulent flow.

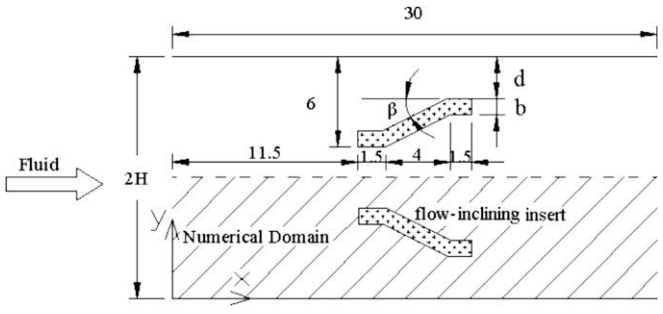


**Fig. 1.** Schematic of the simulated cycle and the numerical domain (unit: mm).

## 2. Mathematical and numerical model

The simulated configuration is a 2-D parallel-plate channel with periodical flow-inclining inserts. To study the fully developed characteristic a cycle of the channel is taken as in Fig. 1. In consideration of the difficulty to form an exact streamlined shape, the quasi-streamlined insert consisting of three straight sections has been adopted here. Due to its symmetrical feature only half of the cycle is considered as the numerical domain. The cycle length is fixed at 30 mm. The half height of the channel $H$ takes 7 mm, 12 mm, and 17 mm respectively. The length of the insert is 7 mm. There are two values, 0.5 and 1 mm, of the plate thickness $b$ to be taken in the numerical study to identify its effect on the flow and heat transfer. The upwind space between the insert and the channel wall is fixed at 6 mm. The downstream space $d$ is variable so that the insert angle $\beta$ can be adjusted. In the simulation the insert angle takes 0°, 8.1°, 16°, 23.2°, and 30° respectively.

For 2-D incompressible steady flow, when the physical property is considered invariable, the governing equations are

$$\frac{\partial u}{\partial x}+\frac{\partial v}{\partial y}=0 \tag{2}$$

$$\rho\left(u\frac{\partial u}{\partial x}+v\frac{\partial u}{\partial y}\right)=-\frac{\partial P}{\partial x}+\mu\left(\frac{\partial^2 u}{\partial x^2}+\frac{\partial^2 u}{\partial y^2}\right)+S_u \tag{3}$$

$$\rho\left(u\frac{\partial v}{\partial x}+v\frac{\partial v}{\partial y}\right)=-\frac{\partial P}{\partial y}+\mu\left(\frac{\partial^2 v}{\partial x^2}+\frac{\partial^2 v}{\partial y^2}\right)+S_v \tag{4}$$

$$\rho C_p\left(u\frac{\partial T}{\partial x}+v\frac{\partial T}{\partial y}\right)=\frac{\partial}{\partial x}\left(k\frac{\partial T}{\partial x}\right)+\frac{\partial}{\partial y}\left(k\frac{\partial T}{\partial y}\right) \tag{5}$$

For the turbulent flow, additional equations are needed to determine the turbulent viscosity and the turbulent Prandtl number. For turbulent flow the standard K–ε model has been adopted. The related equations are

$$\rho\left(u\frac{\partial K}{\partial x}+v\frac{\partial K}{\partial y}\right)=\frac{\partial}{\partial x}\left(\Gamma_k\frac{\partial K}{\partial x}\right)+\frac{\partial}{\partial y}\left(\Gamma_k\frac{\partial K}{\partial x}\right)+S_k \tag{6}$$

$$\rho\left(u\frac{\partial \varepsilon}{\partial x}+v\frac{\partial \varepsilon}{\partial y}\right)=\frac{\partial}{\partial x}\left(\Gamma_\varepsilon\frac{\partial \varepsilon}{\partial x}\right)+\frac{\partial}{\partial y}\left(\Gamma_\varepsilon\frac{\partial \varepsilon}{\partial y}\right)+S_\varepsilon \tag{7}$$

For laminar flow, the source terms $S_u$, $S_v$ and the Equations (6) and (7) are not needed. The detailed expression of the source term and the related turbulent parameters is referred to [4]. The inlet and outlet of the domain are periodic boundary conditions. The principal wall is kept at 350 K. A mass flow given to the inlet corresponded to a Reynolds number. The insert material is copper, and the fluid is water.

The CFD software FLUENT with SIMPLE algorithm has been used in the simulation. The discrete scheme for the momentum and energy equations adopted the second order upwind. The grid independence of the solution has been checked to ensure the accuracy of the numerical result. The typical grid division was $150\times 64$ for $x$ and $y$ direction. The criterion of convergence for terminating the iteration is $10^{-4}$ for the momentum equation and $10^{-6}$ for the energy equation.

The Reynolds number is defined as

$$Re=\frac{u_m\cdot D_e}{\nu} \tag{8}$$

where $u_m$ represents the average velocity at the inlet. The hydraulic diameter of the channel is $D_e = 4H$. The local heat transfer coefficient $h(x)$ is determined by the relationship of the energy balance

$$h(x) = \frac{-k\left(\frac{\partial T}{\partial y}\right)_w}{(T_w - T_b)} \tag{9}$$

$T_b$ is the bulk-averaged temperature of the fluid. The Nusselt number is calculated from the $h(x)$

$$Nu(x) = \frac{h(x)D_e}{k} \tag{10}$$

The average friction factor along the cycle follows the Darcy definition

$$f_m = \frac{\Delta P}{\frac{L}{D_e}\cdot\frac{\rho u_m^2}{2}} \tag{11}$$

where $\Delta P$ is the pressure drop between the inlet and the outlet of the cycle.

## 3. Fields of velocity and temperature

### 3.1. Velocity field

Fig. 2 shows the laminar and turbulent flow field along the main flow direction for $Re = 500$ and $Re = 50{,}000$. Here the flow field is presented with the velocity isolines. For the laminar flow, most fluid flows near the channel centerline rather than through the gap between the insert and the duct wall. On the other hand, the velocity increases locally under the insert because of its inclining function. This indicates the local attenuation of the flow boundary layer. Since the temperature field depends upon the velocity distributions, the variation of the flow field means the change of the heat transfer. For the turbulent flow, though the fluid velocities over the insert are still higher than those under the insert, the distribution of the velocity has become more even comparing to that of the laminar situation. In contrast to the highest velocity of 1.6 m/s in the upper part, the maximum in the lower part is 1.2 m/s. This suggests that the inclining function of the insert is more obvious for the turbulent flow than for the laminar flow. Downstream the insert the flow field can be divided into three districts: the slow insert-trailing part and the two fast regions near the centerline and near the bottom wall. The flow field near the duct wall is the important factor that affects the convection heat transfer, which will be discussed in the following sections.

### 3.2. Temperature field

The temperature fields corresponding to the flow fields shown in Fig. 2 are presented in Fig. 3. Different from the parabolic isotherms in smooth duct, the current isotherms have distorted due to the presence of the flow-inclining insert, especially for the laminar situation. The isotherms tend to cluster onto the duct wall. This suggests that the temperature gradient has been promoted and the heat transfer improved locally. The main difference between the laminar and the turbulent profiles is the uniformity of the isotherms. Comparatively, the isotherm distributes evenly for the laminar flow, while it is much denser near the bottom wall for the turbulent case. This reflects the distinct rules of heat transfer in the two different flow regimes: for laminar convection, the heat transfer resistance spreads across the channel section; but for the turbulent flow, the resistance almost converges to the thin layer adjoining the wall. Correspondingly, approaches to enhance the laminar convection should be applied to the bulk fluid, while they are only considered to disturb the flow near the wall for turbulent situations.

A point worthy to note is the function of the insert. The insert here does not have the conventional function of a real insert, which usually acts as extending surface of heat transfer. Since it is a 2-D channel, the flow-inclining insert does not connect with the channel wall, so there is no path for heat transfer from the wall to the insert. The single function of the insert is just to deflect the fluid onto the channel wall, and improves the degree of the field synergy between the fluid velocity and the temperature gradient.

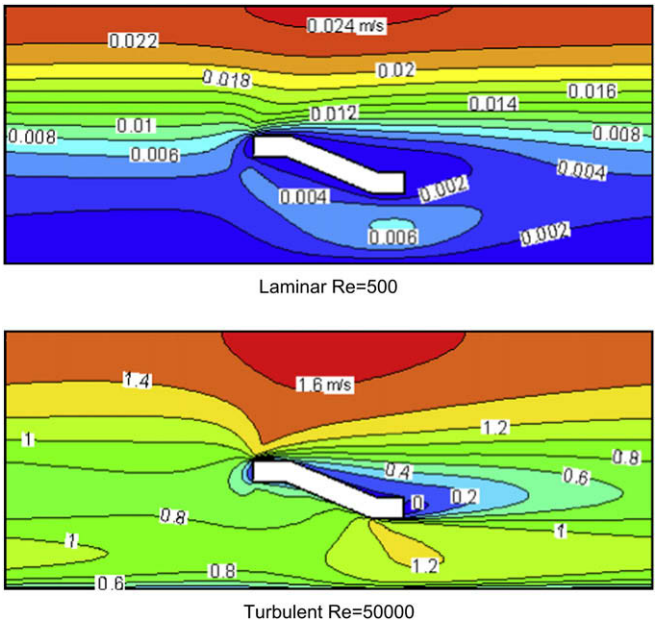


**Fig. 2.** Velocity field ($2H = 24$ mm, $\beta = 23.2°$, $b = 1$ mm).

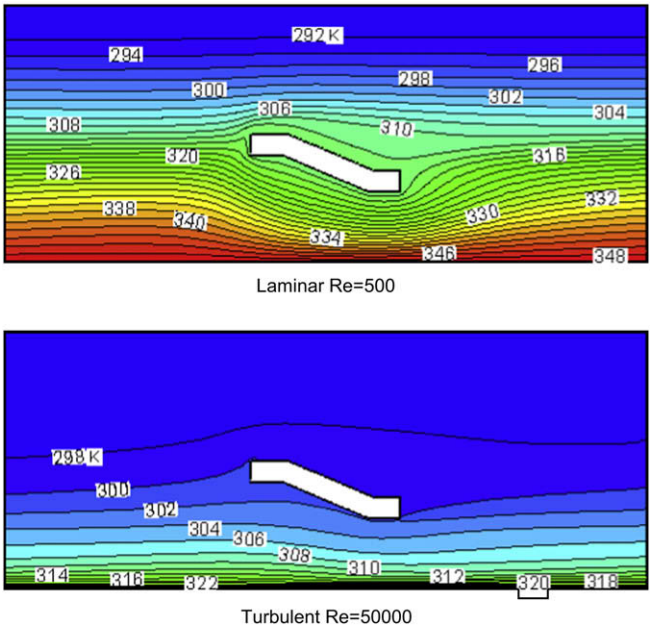


**Fig. 3.** Temperature field ($2H = 24$ mm, $\beta = 23.2°$, $b = 1$ mm).

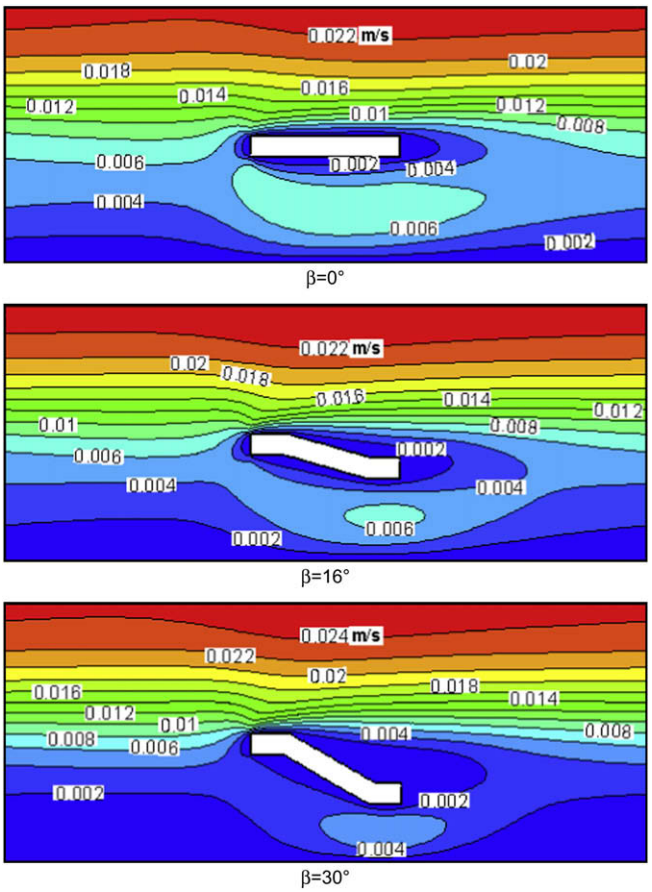


**Fig. 4.** Variation of the velocity fields for different insert angles ($2H = 24$ mm, $b = 1$ mm, $Re = 500$).

### 3.3. Effect of the insert angle on the velocity distribution

The purpose to deploy the flow-inclining inserts is that they cause more fluid to flow towards the channel wall and then improve the field synergy. Small insert angles are no doubt the unappreciated. Whether big insert angles are profitable still remain exploratory. The variation of the velocity distribution with the insert angle can be seen from Fig. 4. In view of briefness, only the profiles of $\beta = 0°$, 16° and 30° are presented. Even for the case of $\beta = 0°$, the flow field also deformed to some extent. This deformation is caused by the thickness of the plate. Therefore the insert thickness is a factor to affect the flow and heat transfer, and its effect will be discussed in the subsequent sections. With the increase of the insert angle, the flow field deforms more strongly. But this does not mean that bigger insert angles always cause more fluid inclining onto the channel wall. Taking account together of the fluid velocity and the quantity flowing through the gap between the insert and the wall, there should be an optimum insert angle that produces the best effect. For the enhanced configuration of 3-D flow-inclining insert in Ref. [10], the experimental result verified that the case of $\beta = 16°$ was the most profitable in most cases. The insert of big angle will block the flow section too much and results in higher pressure-drop, in such a way that it may not be the best option. The current optimum insert angle will be identified when the enhancement effect of the heat transfer is evaluated in the following.

## 4. Characteristics of heat transfer and flow resistance

Though the channel height is an important parameter affecting the heat transfer, the presented results in the following are only for the case of $H = 12$ mm, so that the comparison between the current result and those of the straight flow-inclining insert in Ref. [10] can be conducted readily. The detailed effect of the channel height on the heat transfer can be seen in Refs. [10,11].

### 4.1. The average friction factor

Now the attention is turned to the discussion of the flow and heat transfer characteristics in a cycle. Figs. 5 and 6 show the variation of the average friction factor in a cycle with the Reynolds number. For the results of the laminar flow in Fig. 5, the difference of the friction factors for the enhanced configuration and for the smooth channel is obvious, though they all possess the same declining tendency with *Re*. On the other hand, the insert angle is less influential to the friction of the enhanced channel. The friction discrepancy for different insert angles is hardly distinguished. This feature of the laminar cases quite differs from the turbulent cases, see Fig. 6. For the turbulent flow, the insert angle impacts the friction intensively. The friction discrepancy for different insert angles even exceeds their discrepancy with the smooth channel. The friction factor increases monotonically with the insert angle in turbulent flow. As to the effect of the thickness of the plate $b$, the friction difference for $b = 1$ mm and 0.5 mm is detected in the figure. The thicker insert results in higher flow resistance, especially for the turbulent cases. A simple calculation tells us that the $f_m$ of $b = 1$ mm is 6%–9% higher than that of $b = 0.5$ mm for the laminar flow, but this difference is 33%–62% for the turbulent flow. Therefore, both the insert angle and the insert thickness impact the

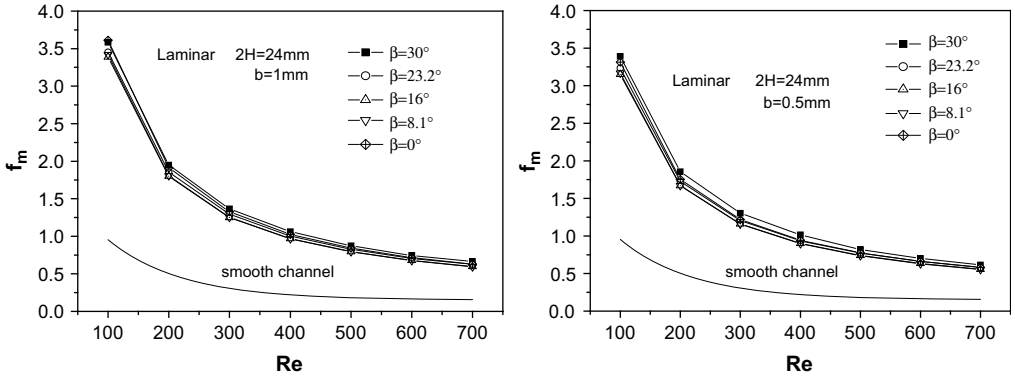


**Fig. 5.** Average friction factor vs Reynolds number for the laminar flow.

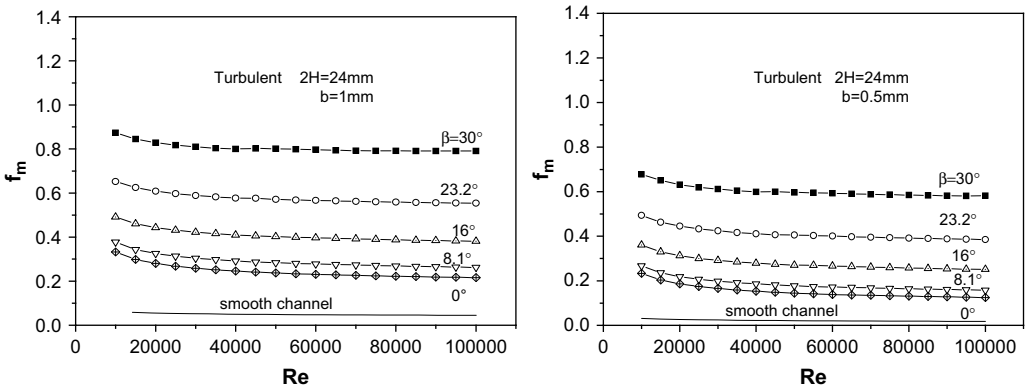


**Fig. 6.** Average friction factor vs Reynolds number for the turbulent flow.

friction characteristic more for the turbulent flow than for the laminar flow.

### 4.2. The average Nusselt number

The cycle-averaged Nusselt number is presented in Fig. 7 for the laminar flow and in Fig. 8 for the turbulent flow. Different from the friction result shown in Fig. 5, the average Nusselt number for the laminar flow in Fig. 7 diverges from each other. The $Nu_m$ increases clearly with the insert angle. Also different from the sagged feature of the laminar friction, the $Nu_m$ here does not change much with the Reynolds number when *Re* is over 400. All of the Nusselt numbers for the enhanced channel are greater than that of the smooth channel. For the turbulent flow, the profiles shown in Fig. 8 are much more aggressive than the laminar cases. The $Nu_m$ difference between the enhanced channel and the smooth one gets great at higher Reynolds numbers. Corresponding to the promoted effect on the friction factor, the big insert angle results in stronger heat transfer, too.

Again, the insert thickness proves to be an influential factor on the heat transfer. For both the laminar and the turbulent flow, the results of $b = 1$ mm are all superiors to those of $b = 0.5$ mm. Nevertheless, the effect of the thickness $b$ on the laminar case seems to be greater than on the turbulent case. This can be interpreted as follows: In addition to the inclining effect of the plate sidewall, the plate front wall also acts as an incliner that promotes the fluid-flow towards the channel wall. The bigger the front wall/plate thickness, the more obvious of the promoting function. Since the heat transfer in laminar flow is less strong as in the turbulent flow, the promoting function of the front wall imposes more effect on the laminar heat transfer than on the turbulent cases. If we combine the heat transfer result in Figs. 7 and 8 and the variation of the friction factor in Figs. 5 and 6, an important conclusion can be drawn: for laminar flow the thicker insert originates higher heat transfer with almost the same pressure-drop penalty as the thinner insert, while for the turbulent flow the thicker insert results in obviously high pressure-drop but does not improve the heat transfer too much. Therefore, in terms of the input and output ratio of a heat exchanger, thicker inserts should be preferred for the laminar flow and thinner inserts preferred for the turbulent flow.

### 4.3. The local Nusselt number

Distributions of the local Nusselt number $Nu(x)$ in a cycle are shown in Fig. 9. To facilitate the comprehension of the $Nu(x)$ variation, the relative position of the insert has also been presented. By the structure of the channel shown in Fig. 1, the insert range covers from $x/L = 0.383$ to 0.617. Though the undulation of the $Nu(x)$ occurs for both the laminar and the turbulent flow, their extents are quite different. The $Nu(x)$ variation for the laminar case is much more drastical than for the turbulent. Because of the undulation there exist a maximum and a minimum of the $Nu(x)$. One can see that the relative location of the peak and the valley with respect to the insert are different for the laminar and for the turbulent. For the laminar flow, the minimum and the maximum occur upstream the leading edge and the trailing edge of the insert respectively. But for the turbulent flow the minimum locates almost at the same site as the leading edge, and the maximum $Nu(x)$ occurs downstream the

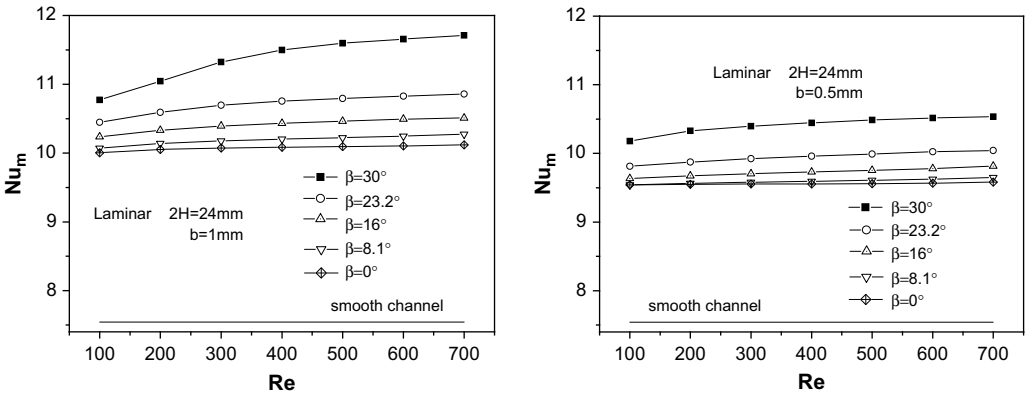


**Fig. 7.** Average Nusselt number vs Reynolds number for the laminar flow.

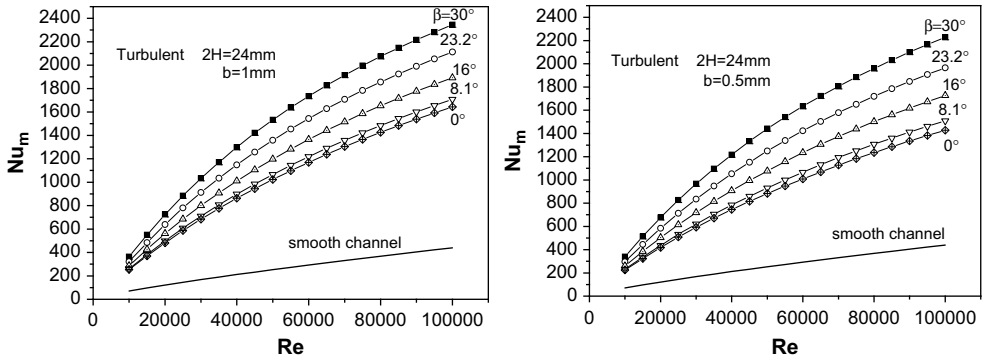


**Fig. 8.** Average Nusselt number vs Reynolds number for the turbulent flow.

trailing edge. As the Reynolds number increases, the turbulent maximum shifts downstream, too. All the maximum of the turbulent flow fall in between $x/L = 0.64$ and $x/L = 0.75$.

As indicated in Fig. 9, the $Nu(x)$ is mainly escalating in the range of the insert. Because of the inclining function of the insert, the velocity component in the normal direction to the channel wall becomes greater and the field synergy between the velocity and the temperature gradient is improved. As a result, the convective heat transfer between the wall and the fluid is augmented. When the fluid flows out of the wall-insert strait, the boundary layer begins to develop once again. This results in the decline of the Nusselt number apart from the insert range. Thus, the flow-inclining insert functions as a local upgrader of the heat transfer.

The dependence of the local Nusselt number on the Reynolds number is also distinctive for the laminar and the turbulent case. Generally, the $Nu(x)$ increases with the Reynolds number for both the cases. On the other hand the $Nu(x)$ depends on the $Re$ more strongly for the turbulent than for the laminar. In the laminar flow, the $Nu(x)$s are almost the same in the upgrading section, and in the other sections the $Nu(x)$s still do not change much with the Reynolds number. This reflects the different characteristics of heat transfer of the laminar and the turbulent flow.

## 5. Evaluation on the enhancement effect

To validate the advancement of the improved streamline insert, a comparison of the heat transfer between the current structure and the original straight insert structure in Ref. [10] is necessary. Variations of the friction factor and the mean Nusselt number for the two structures have been presented in Fig. 10. Since the study in Ref. [10] was only for the turbulent flow, the comparison here is also towards the turbulent case. Obviously, the friction factor of the straight insert is much higher than that of the streamline insert for a given Reynolds number. For the case of $\beta = 23.2^\circ$ the factor of the straight insert is almost two folds of the streamline insert. It is clear that the adoption of the streamline insert decreases the flow resistance drastically. On the other hand, the mean Nusselt number does not differ very much. Though the $Nu_m$ of the straight insert is still over the corresponding streamline value, the difference is moderate. The detailed check reveals that the $Nu_m$ difference of the two insert structures ranges from 6.3% to 15.4%.

The evaluation of the enhancement effect under the constraint of the identical power consumption may be even more convictive, see Fig. 11. The procedure of this evaluation method is referred to [3]. From the results in Fig. 11 we see that the streamline insert is generally superior to the straight insert. Only in the range of $Re = 4 \times 10^4$–$6 \times 10^4$ the enhancement ratios $Nu_m/Nu_0$ for the two configurations are nearly the same. At other Reynolds number the effect of the streamline insert is better than that of the straight insert. The biggest difference reaches 12%.

## 6. Concluding remarks

As continuous work of the study on the enhanced channel of straight flow-inclining insert, an improved quasi-streamline insert is developed and numerically simulated to the periodically developed flow and heat transfer. The current simulation is focused on the effect of the insert angle, the plate thickness, and the Reynolds number. The involved Reynolds number covers both the laminar flow and the turbulent flow. In the range of the insert angle from $\beta = 0^\circ$ to $30^\circ$, the Nusselt number increases with the insert angle monotonically. On the other hand, the insert angle is less influential

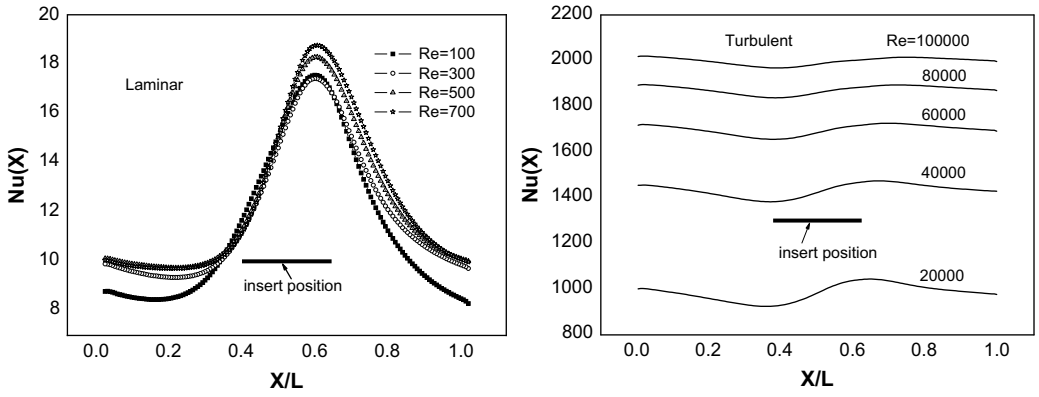


**Fig. 9.** Variation of the local Nusselt number in a cycle at different Reynolds numbers ($2H = 14$ mm, $b = 1$ mm, $\beta = 23.2^\circ$).

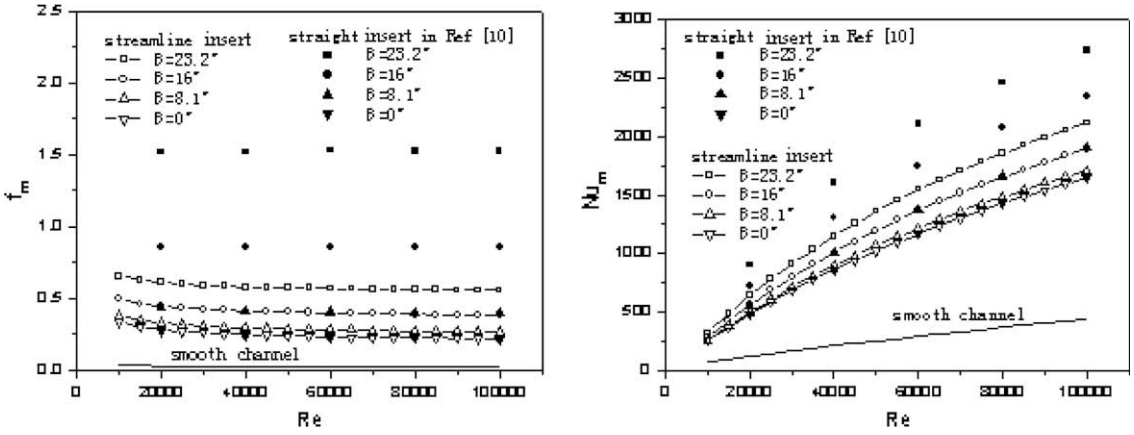


**Fig. 10.** Comparison of the friction and heat transfer to the results of the enhanced channel of straight insert ($2H = 24$ mm, $b = 1$ mm).

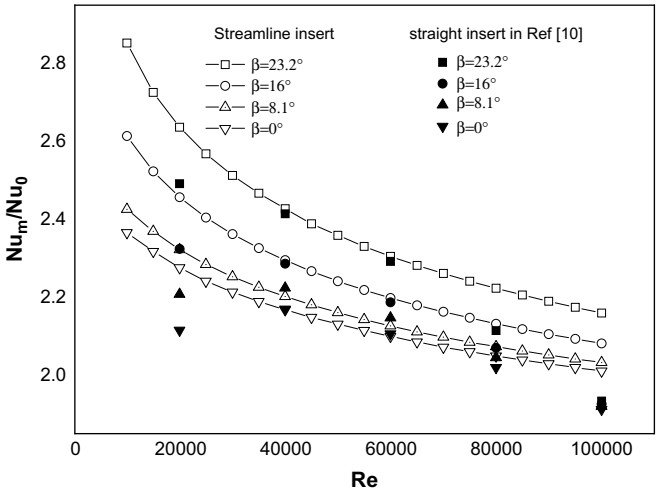


**Fig. 11.** Evaluation of the thermal performance under the identical pump power consumption ($2H = 24$ mm, $b = 1$ mm).

to the flow resistance of the laminar case than to the turbulent case. The plate thickness also shows different effect on the characteristics of the heat transfer and the flow resistance. Taking account of the heat transfer and the pressure-drop together, the thicker insert is recommended to apply in the laminar flow and the thinner insert to the turbulent flow.

The numerical results reveal that the distribution of the local Nusselt number changes with the Reynolds number in the laminar case not as drastically as in the turbulent case. In any case, the flow-inclining insert functions as a local upgrader of the heat transfer and is capable of pumping up the declining heat transfer coefficient. The insert causes the improvement of the field synergy between the fluid velocity and the temperature gradient. Furthermore, the result indicates that the adoption of the streamline insert decreases the flow resistance but with only a moderate deterioration of the heat transfer. When evaluated under the constraint of the identical pump power consumption, the configuration of the streamline insert exhibits its superiority to the straight insert. The difference of the enhancement ratio $Nu_m/Nu_0$ for the two configurations reaches 12%.

## Acknowledgement

This work is sponsored by Beijing Natural Science Foundation (3052002), and National Natural Science Foundation of China (50876003).

## References

[1] H.T. Cui, X.G. Yuan, Z.P. Yao, Y.F. Zhu, Experimental investigation on the heat transfer and flow resistance characteristics of a special-shaped spirally fluted tubes. In: Proceedings of the CSEE, vol. 23, no. 6; 2003. p. 217–220.
[2] E.M. Sparrow, W.Q. Tao, Symmetric vs asymmetric periodic disturbances at the walls of a heated flow passage, Int J Heat Mass Transfer 27 (11) (1984) 2133–2144.
[3] Z.X. Yuan, W.Q. Tao, Q.W. Wang, Numerical prediction for laminar forced convection heat transfer in parallel-plate channels with streamwise-periodic rod disturbances, Int J Numer Methods Fluids 28 (1998) 1371–1387.
[4] Z.X. Yuan, Numerical study of periodically turbulent flow and heat transfer in a channel with transverse fin arrays, Int J Numer Methods Heat Fluid Flow 10 (8) (2000) 842–886.
[5] Z.Y. Guo, D.Y. Li, B.X. Wang, A novel concept for convective heat transfer enhancement, Int J Heat Mass Transfer 41 (1998) 2221–2225.
[6] S. Wang, Z.X. Li, Z.Y. Guo, Novel concept and device of heat transfer augmentation. In: Proceedings of 11th IHTC, vol. 5; 1998. p. 405–8.
[7] W.Q. Tao, Z.Y. Guo, B.X. Wang, Field synergy principle for enhancing convective heat transfer - its extension and numerical verifications, Int J Heat Mass Transfer 45 (2002) 3849–3856.
[8] Z.X. Yuan, J.G. Zhang, M.J. Jiang, Analytical study on coordinative optimization of convection in tubes with variable heat flux, Sci China Ser E 47 (6) (2004) 651–658.
[9] J.A. Meng, Z.J. Chen, Z.X. Li, Z.Y. Guo, Experimental and numerical study on heat transfer and flow resistance in alternating elliptical axis tubes, J Eng Thermophysics 25 (5) (2004) 813–815.
[10] Z.X. Yuan, L.H. Zhao, B.D. Zhang, Fin angle effect on turbulent heat transfer in parallel-plate channel with flow-inclining fins, Int J Numer Methods Heat Fluid Flow 17 (1) (2007) 5–19.
[11] L.H. Zhao, B.D. Zhang, Z.X. Yuan, Investigation on periodically developed heat transfer in a specially enhanced channel, Heat Mass Transfer 44 (2008) 287–296.